

ACI STRUCTURAL JOURNAL

A JOURNAL OF THE AMERICAN CONCRETE INSTITUTE

Prepublished Paper

This is a prepublished manuscript. The final manuscript is tentatively scheduled for V. 121, No. 4 and is subject to change.

The DOI for this paper is 10.14359/51740571 and will not change, but won't be activated until the issue has been published.



DESIGN METHODOLOGY FOR UNBONDED POST-TENSIONED ROCKING WALLS

Qingzhi Liu^{1,2}, Catherine French², Sri Sritharan³

Biography:

ACI member **Qingzhi Liu** is a Structural Engineer at WSP-Englekirk, Los Angeles, CA. He received his BS from South China University of Technology, Guangzhou, China; MS from Tsinghua University, Beijing, China; and PhD from the University of Minnesota, Twin Cities. He is a member of ACI Committee 550 and involved in Committee 374 and 239. His research interest includes resilient precast concrete structures, performance-based design and ultra-high-performance concrete (UHPC).

Catherine W. French is CSE Distinguished Professor at the University of Minnesota, Twin Cities, MN. She received her BCE from University of Minnesota, Twin Cities; MS and PhD from University of Illinois at Urbana-Champaign. She is a member of ACI Technical Activities Committee (TAC), 318, 352, and 445. Her research interests include experimental and numerical investigations of the behavior of reinforced concrete structural systems including time-dependent, environmental, and earthquake effects and development of new materials.

FACI member **Sri Sritharan** is the Wilkinson Chair Professor and Assistant Dean in the College of Engineering and Professor of Structural Engineering in the Department of Civil, Construction and Environmental Engineering at Iowa State University, Ames, IA. He is a former Chair of ACI

¹ WSP-Englekirk, Los Angeles, CA, 90017

² Department of Civil, Environmental, and Geo- Engineering, University of Minnesota, Twin Cities, MN, 55455

³ Department of Civil, Construction and Environmental Engineering, Iowa State University, Ames, IA, 50011

Committee 341 (Earthquake-Resistant Concrete Bridges) and a member of ACI Committees 341 and 447 (Finite Element Analysis of Reinforced Concrete Structures). His research interests include the design of concrete structures and earthquake engineering.

Abstract:

Unbonded post-tensioned rocking walls have demonstrated superior seismic performance with greatly reduced damage and excellent self-centering behavior. Current design guidelines (ACI-550.7) and representative research on rocking walls are summarized in this paper. Some inconsistencies and voids in the major design parameters for rocking walls are identified. A brief description is provided for two rocking-wall specimens tested under quasi-static cyclic loading. Force flow and failure mechanisms of rocking walls observed from the tests were studied, and it is discovered that they are very different from those of special structural walls. The test data showed that concentration of compressive strain in concrete at the corners of rocking walls was a local behavior such that the need for confinement reinforcement higher above the toe region was diminished. Fiber grout weaker than concrete in rocking walls used as ductile bearing materials at wall-foundation interface is a reasonable alternative to ACI-550.7. Design recommendations for height and volumetric ratio of confinement reinforcement are provided. A requirement for the aspect ratio of rocking walls stricter than that in ACI-550.7 is proposed to prevent shear-sliding of the walls.

Subject Headings: Rocking wall, Precast, Seismic, Aspect ratio, Confinement reinforcement

Introduction

Specific design guidelines for the innovative rocking walls are not included in “Building Code Requirements for Structural Concrete” (ACI 318, 2019), but these systems are permitted in practice according to Section 18.11.2.2: “Special structural walls constructed using precast concrete and unbonded post-tensioned tendons are permitted provided they satisfy the requirements of ACI ITG-5.1.” ITG-5.1 was later incorporated into ACI 550.7 - “Requirements for Design of a Special Unbonded Post-Tensioned Precast Shear Wall Satisfying ACI-550.6 (ACI 550.7) and Commentary.” Due to limited experimental and analytical studies at the time of developing the document, ACI-550.7 is not entirely complete (e.g., recommendations for height and volumetric ratio of confinement reinforcement are not included). In this paper, a brief comparison of the major design parameters of rocking walls recommended in ACI-550.7 and used in existing tests is presented first. Next, the mechanism of rocking walls is described using results from two rocking-wall specimens tested by the authors. Based on the study, more complete recommendations for the design parameters of rocking walls are provided.

As shown in Fig. 1, the major design parameters of rocking walls discussed in this paper include: aspect ratio (height-length ratio), shear-sliding resistance, confinement reinforcement, and grout bearing at wall-foundation interface. Table 1 lists the major design parameters of rocking walls recommended by ACI-550.7 and used in existing studies. The five referenced tests include: A 5/12-scale, four-story isolated rocking wall (TW1) tested at Lehigh University (“LEHIGH,” Perez 2004); a 1/2-scale, three-story rocking-wall structure tested at University of California, San Diego (“DSDM,” Schoettler 2010); a 1/2-scale, six-story rocking wall tested at National Center for Research on Earthquake Engineering (“NCREE,” Aaleti and Sritharan 2011); a full-scale, four-

story rocking-wall structure tested on E-Defense shake table in Japan (“E-DEFENSE,” Gavridou et al. 2017); two 1/3-scale, six-story rocking-wall specimens tested at University of Minnesota, Twin Cities (“PFS1” and “PFS2,” Liu et al. 2016). A brief summary of each design parameter is provided below.

Aspect ratio - Section 5.4.2 of ACI-550.7 recommends that rocking walls should have an aspect ratio equal to or greater than 0.5. All referenced tests satisfied this requirement.

Shear-sliding resistance - Section 6.5.3 of ACI-550.7 suggests that nominal shear-sliding resistance shall be taken as μC , where C is the compression force acting on the interface and μ is coefficient of friction taken as 0.5. The shear-sliding resistance shall be greater than the base shear associated with M_{pr} , where M_{pr} is the probable flexural strength of the wall. This methodology was adopted in all referenced tests. In this paper, shear-sliding behavior of rocking walls is further studied with regard to aspect ratio of the walls.

Grout layer underneath the wall - Section 6.8 of ACI-550.7 suggests that steel or polypropylene fiber shall be added to grout bearing to increase its toughness; the specified strength of the grout shall be larger than the greater of f'_c , and $0.4f'_{cc}$, where f'_c and f'_{cc} are the strength of unconfined and confined concrete in the walls, respectively. The code requirements were satisfied in the “LEHIGH” test with nylon-fiber-reinforced grout (7.5 ksi [52 MPa]) stronger than unconfined concrete in the wall (6 ksi [41 MPa]). In the “NCREE” test, steel-fiber-reinforced grout with 14 ksi (97 MPa) strength was used, which was slightly larger than the actual strength of confined concrete in the wall (13 ksi [90 MPa]). Negligible damage occurred to the grout in both tests. The grout used in the “E-DEFENSE” test (either with fiber: 17.4 ksi [120 MPa] or without fiber: 19.7 ksi [136 MPa]) was stronger than the unconfined concrete in the wall (12.3 ksi [85 MPa]). The

fiber-reinforced-grout used underneath the north rocking wall remained intact, but the grout without fiber used underneath the south rocking wall was crushed, spalled and partly fell out during early stages of testing (Gavirou et al. 2017).

Although it is not recommended in ACI-550.7, fiber-reinforced grout turned out to be weaker than unconfined concrete in the wall in some tests, which provided some insights different from the code. In the “DSDM” project, polypropylene-reinforced-grout with 7 ksi (48 MPa) strength was used, which was weaker than unconfined concrete in the wall (7.8 ksi [54 MPa]). Minor crushing of the grout was observed in the test (Belleri et al. 2014). In the “PFS1” and “PFS2” tests, steel-fiber-reinforced grout (8.7 ksi [60 MPa]) was weaker than unconfined concrete in the wall (11.2 ksi [77 MPa] in PFS1, 10.4 ksi [72 MPa] in PFS2). Further discussion of the grout bearing is provided later in the paper.

Confinement reinforcement - Section 6.6.3.6 of ACI-550.7 recommends that the confinement reinforcement in the compressed concrete should satisfy 18.10.6.4(e) of ACI 318-14 (detail and spacing of confinement); the confinement should extend horizontally from the extreme concrete compression fiber a distance not less than $0.95c$ or 12 in. (305 mm), where c is neutral axis depth of the wall (length of confinement). There are no specific requirements provided for the height or volumetric ratio of confinement reinforcement in the document. In the “LEHIGH” test, design of the confinement reinforcement was mainly based on the requirements for special structural walls in ACI 318. Design philosophy for the confinement reinforcement in the wall was not found in the literature for the “E-DEFENSE” test. In “DSDM,” “NCREE,” “PFS1,” and “PFS2” tests, the volumetric ratio of confinement reinforcement was designed to ensure that the maximum strain in the extreme concrete compression fiber (ϵ_{cc}) could be developed at the target drift. Different

equations were proposed to predict ϵ_{cc} . In the “NCREE,” “PFS1,” and “PFS2” tests, ϵ_{cc} was associated with neutral axis depth of the wall (c), target drift (θ), elastic curvature of the wall (ϕ_e), and height of wall (H) in the equation $\epsilon_{cc} = c(\phi_e + \theta/(0.06H))$ (Aaleti and Sritharan 2011). It was empirically assumed that the height of an “equivalent” plastic hinge in rocking walls was $0.06H$, and plastic curvature of the walls [$\theta/(0.06H)$] was constant over the plastic hinge. In the “DSDM” project, it was assumed that ϵ_{cc} was distributed over a distance equal to c along height of the wall, and thus ϵ_{cc} was equal to θ ($\epsilon_{cc} = \theta c/c = \theta$). For length of confinement reinforcement, ACI-550.7 was followed in the “NCREE,” “PFS1,” and “PFS2” tests. It was empirically decided to extend the confinement 12 in. (305 mm) horizontally from wall ends in the “DSDM” test. Height of confinement reinforcement was also selected empirically in the “DSDM” test, while it was equal to the wall length in the “NCREE” test based on the requirements for special structural walls in ACI 318. In the “PFS1” and “PFS2” tests, the height of confinement reinforcement was equal to 47% and 56% of the wall length, respectively. They were selected based on the “NCREE” test, after which a smaller height of confinement reinforcement was recommended compared to special structural walls.

Research Significance

The design parameters (height and volumetric ratio) for confinement reinforcement in rocking walls are not included in ACI-550.7 and vary greatly among different tests. The grout bearing has a non-negligible impact on these design parameters. The aspect ratio of rocking walls is associated with their shear-sliding resistance. These are critical design parameters for engineers in practice. A rational methodology, which is based on different grout conditions and subsequently determines

different requirements for the confinement reinforcement in rocking walls, is introduced. A requirement for aspect ratio of the walls that is stricter than current design guideline is provided.

Experimental Program

Two specimens (“PFS1” and “PFS2”), which were 1/3-scale from a six-story office building, were tested by the authors. Quasi-static cyclic loading was applied to the top of the specimens under displacement control. Detailed descriptions of the tests can be found in the literature (Liu 2016). Multiple concrete and steel strain gages were installed in the walls, which provided useful data to study the strain distribution in rocking walls. Fig. 2 shows the concrete (CG) and steel reinforcing (SG) strain-gage layout in the walls. Readings from the concrete strain gages are direct measurements of local compressive strains, while readings from the steel strain gages attached to the stirrups reveal confinement effect, which is an indirect indicator of the concrete compressive strains in the wall.

The strain-gage readings recorded at different lateral drift levels of the wall (0.1%, 0.5%, 2%, 3%, 4% and 5%) were used for the study. It was observed that the walls were not uplifted until 0.25% drift, thus the results at 0.1% drift represented the condition before rocking of the walls. The 0.5% drift was selected as the drift limit under service-level earthquakes. The 2% drift was associated with design-level earthquakes. Per Section 5.3.4 in ACI-550.7, the limiting drift required for rocking walls is 3% under maximum-considered earthquakes (MCE). Although it is beyond the code requirement, the rocking-wall structures can sustain drifts larger than 3%, and the results at 4% and 5% drifts were also used. During the tests, readings from some concrete strain gages became very large at 5% drift, after spalling of the concrete surrounding the gages occurred. Despite the data being beyond the nominal measurement range specified in the product manual

(20000 $\mu\epsilon$), it is still presented to provide some insight regarding large strains that could be developed locally.

Disturbed and undisturbed region in the wall panel - Fig. 3(a) shows the concrete compressive-strain distribution along the length of the wall near the base of PFS1; data with negative signs represent compressive strains. As shown in the figure, strain compatibility was not valid (i.e., plane sections did not remain plane) across the length of the wall, especially after uplift of the wall (0.5% to 5% drift): large compressive strains concentrated at the wall corners; strains were very small in the uplifted side of the wall. Strain distribution was approximately linear over the compression zone. Similar conclusions can be drawn based on the test results from PFS2. Fig. 3(b) and (c) show the concrete compressive-strain distribution along the length of the wall near the base and at 18 in. (457 mm) from the base. As shown in the figures, strain compatibility was invalid at these cross sections of the wall. Fig. 3(d) shows the concrete compressive-strain distribution at 148 in. (3759 mm) from the base. As shown in the figure, strains were distributed approximately linearly across the length of the wall, and thus strain compatibility was valid at this section (i.e., it was not disturbed). Therefore, a disturbed region existed in the wall near the wall-foundation interface; the compression force concentrated where the wall contacted the foundation.

Fig. 4(a) shows the concrete compressive-strain distribution along the height of the wall within 10 in. (254 mm) from the base in PFS1. As shown in the figure, the strain greatly decreased along the height of the wall, especially at larger drifts. At 3% drift, the compressive strain was 1760 $\mu\epsilon$ at the base (CG-W5 in Fig. 2(a)), but it decreased to 980 $\mu\epsilon$ at 8 in. (203 mm) above the base (CG-W6). At 5% drift the strain at CG-W5 grew up to 25750 $\mu\epsilon$, but it rapidly decreased to 1360 $\mu\epsilon$ at CG-W6, which was smaller than the maximum usable strain of unconfined concrete (3000 $\mu\epsilon$)

specified in ACI 318-19. This was in accordance with the test observation that the damage was concentrated near the base of the wall (measured as 7.5 in. [191 mm]), where CG-W5 was included but not CG-W6 as shown in Fig. 2(a). Similar behavior was observed in PFS2. As shown in Fig. 4(b), the compressive strain was $3190 \mu\epsilon$ at the base (CG-W1 in Fig. 2(b)) at 3% drift, but it decreased to $1230 \mu\epsilon$ at 10 in. (254 mm) above the base (CG-W7). The rate of decrease was reduced further away from the base of the wall, as the compressive strain was $1020 \mu\epsilon$ at 18 in. (457 mm) above the base (CG-W8). At 5% drift, the compressive strain at CG-W1 grew to $53900 \mu\epsilon$, which greatly exceeded the nominal measurement range. The compressive strain rapidly decreased to $2390 \mu\epsilon$ at CG-W7 and $1040 \mu\epsilon$ at CG-W8. Again, this was in accordance with the test observation that concrete spalling occurred within 9 in. (229 mm) above the base of the wall in PFS2, where CG-W1 was included but not CG-W7 or CG-W8 as shown in Fig. 2(b). These observations demonstrated that the compression force rapidly distributed across the length of the wall in the disturbed region with increased height, and strain concentration in the wall corners was a local behavior.

Height of disturbed region - As shown by the test results of PFS2, strain compatibility was not valid at the wall section 18 in. (457 mm or $0.3W$) above the base, but it was valid at the wall section 148 in. (3759 mm or $2.2W$) above the base. The wall length W was equal to 68 in. (1727 mm) in PFS2. The height of the disturbed region was expected to be in between these distances. Based on St. Venant's Principle, the disturbed region would extend to an approximate height of $1.0W$ from the base. The assumption was in line with the test observation.

It is noteworthy that confinement reinforcement is not necessarily required within the entire disturbed region. The tensile strains in the confinement reinforcement in PFS1 and PFS2 were

obtained from the steel strain gages attached to the stirrups in the walls (SW_W1 to SW_W6, shown in Fig. 2). Fig. 5(a) and (b) show the tensile-strain distribution in the stirrups along height of the wall in PFS1 and PFS2, respectively. As shown in the figures, the tensile strains in the stirrups located beyond 10 in. (254 mm) from the base were very small even at large drifts (i.e., 4% and 5%) when concrete compressive strains were large at the wall corners and spalling of concrete occurred, indicating that the confinement reinforcement was only effective over a small region. It further validated that the compression force concentrated toward the wall corner was distributed across the length of the wall, and the concrete compressive strains decreased rapidly along the height of the wall. The behavior observed in rocking walls is very different from that in special structural walls with bonded reinforcement and strain compatibility, as described in detail in the following.

Comparison of Rocking Walls and Special Structural Walls

Fig. 6 shows a comparison of stress distribution and force flow near the base in a rocking wall with those in a special structural wall (assuming the walls are elastic for illustrative purposes). In a rocking wall, tensile resistance is primarily provided by unbonded PT strands. The tensile forces in the PT strands and the associated compressive forces in concrete are constant along the height of the wall. The internal moment distribution along the height of the wall is generated by a change in the distance between the tension-compression ($T-C$) couple, as shown in Fig. 6(a). Because the location of the PT strands in the wall is fixed, the horizontal distribution (i.e., length) of the concrete compression zone increases along the height of the wall to correspond with the relocation of the resultant compression force with height (i.e., reduction of moment). It explains the aforementioned test observation that the concentrated compression force at the wall corners spread

across the length of the wall and the associated compressive strains rapidly decreased with height. Similar conclusions can be made when lateral displacements of the wall become larger, and plasticity occurs in the concrete. Because compressive strains rapidly decrease with height, damage to the concrete is limited locally and confinement reinforcement is mainly used to confine the concrete toward the base in the corners of a rocking wall.

In a special structural wall, tensile resistance is primarily provided by longitudinal reinforcement that is bonded to the surrounding concrete, as shown in Fig. 6(b). The internal moment distribution along the height of the wall is mainly generated by a change in the tensile forces in the reinforcement and the associated compressive forces in the concrete. Generally, change in the distance between the $T-C$ couple is not significant along the height of the wall (i.e., the neutral axis depth remains relatively constant). When lateral displacements of the wall become larger, a plastic hinge, with height generally assumed to be equal to the length of the wall, is formed at the bottom of the wall. Yielding of longitudinal reinforcement and damage to the concrete extend over the entire plastic-hinge region, which has been proven to be much larger than the damaged area in rocking walls (Aaleti 2011, Gavridou et al. 2017). Confinement reinforcement is used not only to confine the concrete, but also to restrain buckling of the yielded longitudinal reinforcement in the plastic-hinge region of a special structural wall.

The other difference between the two types of walls is at wall-foundation interface. A special structural wall is rigidly connected to the foundation, while a rocking wall sits on a grout bed above the foundation. Different from the special structural wall, design of the boundary elements in the rocking wall is also affected by the grout bearing. Shear-sliding behavior at the wall-foundation interface is also different for the two types of walls. In a special structural wall, dowel rebar exists

between the wall and the foundation, and dowel action is a significant source of shear-sliding resistance. In practice, shear sliding of a special structural wall is generally not a governing design factor. On the other hand, shear-sliding resistance is an important design parameter for a rocking wall. Due to discontinuity at the base, shear-sliding resistance of the rocking wall is mainly provided by friction resistance between the wall and the grout (i.e., no dowel action).

To conclude, the force flow and the failure mechanisms of rocking walls are greatly different from those of special structural walls. As expected, some design requirements developed for special structural walls in ACI-318 are not suitable for rocking walls.

Design of Rocking Walls

Grout bed and confinement reinforcement - Due to direct contact, the grout bed underneath the rocking wall has a great impact on the compressive strains developed in the wall corners, which is directly related to the design of the confinement reinforcement in the boundary elements. During construction of PFS1, a pocket was reserved in the foundation to receive the wall. As shown in Fig. 2(a), a layer of fiber grout was poured into the pocket with the wall in place, ensuring a smooth contact at the base. This detail is appealing as it simplifies the erection process and prevents shear sliding of the wall. An alternative wall-foundation interface was adopted in PFS2. As shown in Fig. 2(b), the fiber grout was cast directly onto the foundation (i.e., no pocket). It simplified the prefabrication of the foundation since there was no need to form a pocket at the top. It was deemed cost effective per feedback from the precast industry.

ACI-550.7 recommends that the strength of the grout shall be larger than the greater of f'_c and $0.4f'_{cc}$. The intent was to prevent any damage to the grout because replacing the damaged grout was considered difficult. In the tests of PFS1 and PFS2, the fiber grout was originally designed to

be stronger than the concrete in the wall (i.e., grout: 13 ksi [90MPa], concrete: 6 ksi [41MPa]). However, material tests showed that the actual strength of the grout (8.7 ksi [60MPa]) was weaker than that of the concrete (11.2 ksi [77Mpa]). Learning from precasters, the over-strength of concrete in precast walls is commonplace in the industry. Because precasters desire a fast turnaround time on the precasting bed to produce more products, using high early-strength concrete facilitates the production. On the other hand, the fiber grout was mixed on site using handheld blenders during construction of the two test specimens. Several grout samples made before the tests revealed that some steel fibers settled to the bottom, which reduced the strength of the fiber grout. Considering the difference in quality control and the popularity of high-strength concrete in the precast industry, it is conceivable that the concrete in the precast walls could turn out to be stronger than the fiber grout in practice. It is meaningful to develop some design recommendations for confinement reinforcement in rocking walls with weaker grout, which supplements the current design code ACI-550.7.

As shown in Fig. 5, the maximum stirrup tensile strains near the base of the wall were 260 and 720 $\mu\epsilon$ at 3% drift cycle in PFS1 and PFS2, respectively. These small stirrup tensile strains indicated that the confinement reinforcement was not fully engaged. The strength of the grout underneath the wall was approximately 0.76 times that of the concrete in the wall. Therefore, the grout plastified, and it resulted in an extended neutral axis depth of the wall and reduced the compressive strains developed in the boundary elements of the wall. As shown in Fig. 3, the maximum concrete compressive strains measured at 3% drift cycle were 1760 and 3190 $\mu\epsilon$ in PFS1 and PFS2, respectively. They were either smaller than or close to the maximum usable strain of unconfined concrete (3000 $\mu\epsilon$, ACI 318-19). Similarly, small concrete compressive strains (e.g.,

1560 $\mu\epsilon$ in the wall corners at design-level earthquakes) were observed in the DSDM project (Belleri et al. 2014), where the grout bearing was weaker (i.e., actual compressive strength of concrete in the wall was 1.16 times that of grout).

It is well recognized that confinement reinforcement becomes effective only when lateral expansion of the concrete in compression (i.e., Poisson effect) increases as the concrete experiences large inelastic axial strains. Because the confinement reinforcement provides passive confining effect, it is generally deemed ineffective until the compressive strains in the concrete exceed the maximum usable strain (e.g., 3000 $\mu\epsilon$). With the weaker grout, the development of concrete compressive strains was not significant and steel confinement was not very effective at the 3% drift. These tests demonstrate successful performance of rocking walls with an alternative to ACI-550.7 (i.e., grout weaker than concrete in the wall), which has the benefit of reducing damage to rocking walls at design drifts. It is essential to ensure the grout materials are ductile (e.g., reinforced by steel or polypropylene fiber), such that they would not be lost due to deterioration or crushing, preventing excessive losses of PT forces in the walls due to shortening of the prestressed strands.

As shown in Fig. 3, the concrete compressive strains in both “PFS1” and “PFS2” tests increased at larger drifts (e.g., PFS1: 2750 $\mu\epsilon$, PFS2: 4560 $\mu\epsilon$ at 4% drift) and exceeded the nominal measurement range of concrete strain gages (20000 $\mu\epsilon$) at 5% drift (e.g., PFS1: 25750 $\mu\epsilon$, PFS2: 53900 $\mu\epsilon$), when spalling of concrete cover occurred at the wall corners in both tests. As shown in Fig. 5(a) for PFS1, the stirrup tensile strains rapidly increased from 290 $\mu\epsilon$ at 4% drift to 1540 $\mu\epsilon$ at 5% drift. As shown in Fig. 5(b) for PFS2, the stirrup tensile strains also increased from 680 $\mu\epsilon$ at 4% drift to 880 $\mu\epsilon$ at 5% drift. As demonstrated by the tests, large compressive strains were still

generated at higher drifts even with weaker grout. Although 3% is the drift limit for rocking walls per current design code ACI-550.7, peak transient drift of the buildings might exceed 3% due to variations in ground motions. To ensure their performance comparable to that of monolithic walls under extreme events, the volumetric-ratio requirements for the confinement reinforcement in special structural walls specified in ACI 318 should be implemented to rocking walls with weaker grout (i.e., Table 18.10.6.4 (g)). The height of the confinement reinforcement shall follow the recommendations developed for rocking walls with stronger grout, which are discussed below.

Table 2 summarizes the data collected from the “LEHIGH,” “NCREE,” and “E-DEFENSE” tests, where stronger grout was used, including: height of the region from base of the wall where spalling of concrete cover was observed (Δ), thickness of wall (t), neutral axis depth measured from center of the confinement reinforcement (c), concrete compressive strain measured at prescribed height in the confined region (ϵ_{cc}), stirrup tensile strain measured at prescribed height (ϵ_t , measured by steel strain gages), and the target drift when the measurements were collected. The data ϵ_{cc} from the “LEHIGH” and “NCREE” tests in Table 2 were directly measured by concrete strain gages and the gage length was around 1.2 in. (30 mm) to 4.9 in. (125 mm), over which the measured strains were averaged. In the “E-DEFENSE” test, displacement transducers with 9.8 in. (250 mm) gage length were placed between the corner of the walls and the foundation (Gavridou et al. 2017). The data ϵ_{cc} was obtained by dividing the measured displacement over the gage length.

Height of confinement reinforcement h_{cc} - As shown in Table 2, spalling of concrete cover occurred over a short distance from the base at wall corners in all three referenced tests (Δ is small). Similar behavior had been reported in other rocking-wall tests (Priestley et al. 1999, Restrepo and

Rahman 2007, Henry 2011, Smith 2012). As described above, compressive strains in concrete decrease rapidly along the height of rocking walls due to increased length of concrete compression zone across the walls. Because strain concentration at wall corners is only a local behavior, the confinement reinforcement should be placed between the wall base and a cut-off section, where the strain in the extreme concrete compression fiber is equal to the maximum usable strain of unconfined concrete (e.g., $3000 \mu\epsilon$). Based on the data listed in Table 2, it is recommended that confinement reinforcement should be placed over a height (h_{cc}) not less than 2 times wall thickness ($2t$) or 1.5 times neutral axis depth of the wall ($1.5c'$) at target drifts, whichever is greater. The recommendation of h_{cc} is further discussed.

As shown in Table 2, when the grout bearing was stronger than the concrete in the walls, large concrete compressive strains developed at the wall corners at 3% drift (e.g., $23000 \mu\epsilon$ in the “E-DEFENSE” test). This behavior was different from that observed in the “PFS1” and “PFS2” tests, where weaker grout was used, and concrete compressive strains were close to $3000 \mu\epsilon$ at 3% drift. In all three referenced tests in Table 2, the concrete compressive strain was smaller than $3000 \mu\epsilon$ and the stirrup tensile strain was small in the walls beyond the recommended height of h_{cc} . This matched the observation that spalling of concrete cover in the referenced tests occurred over a short distance from the wall base, listed as Δ in the table. For example, in the “NCREE” test, spalling of concrete cover was observed about 10 inches (254mm) from the base; h_{cc} was calculated as $\max(2 \times 6, 1.5 \times 9.8) = 14.7$ in. (373 mm). The concrete compressive strain measured at 15 in. (381 mm) from the base was $2080 \mu\epsilon$, which was less than $3000 \mu\epsilon$. The stirrup tensile strain measured at 13 in. (330 mm) from the base was only $560 \mu\epsilon$. It was expected that the value

would further decrease at 14.7 in. (373 mm, h_{cc}) from the base, thus the stirrups would not be very effective beyond this elevation.

It is noteworthy that the recommended height of confinement reinforcement in a rocking wall is much smaller than that in a special structural wall, where confinement reinforcement is required over a height not less than length of the wall (ACI 318, 2019). For example, for the rocking wall in the “NCREE” test that was 72 in. (1829 mm) long, 6 in. (152 mm) thick and had a neutral axis depth of 9.8 in. (249 mm) at 3% target drift, the required height for confinement reinforcement h_{cc} would be 14.7 in. (373 mm). On the other hand, the minimum height of confinement reinforcement in a special structural wall would be 72 in. (1829 mm) per ACI 318. As described above, the confinement reinforcement in a special structural wall is used not only to confine the concrete, but also to resist buckling of the yielded longitudinal reinforcement in plastic hinge regions. However, the “equivalent” plastic-hinge concept for a rocking wall is very different from the one generally acknowledged for a special structural wall. Buckling of the longitudinal reinforcement in rocking walls might not be problematic because the longitudinal reinforcement does not yield in tension, and it contributes little to the strength of the walls. Instead, the pretension in the PT strands is the main contributing source to the strength of rocking walls, and their elongation occurs over the full unbonded length, which is generally equal to the entire height of the wall. Rotation of the rocking wall concentrates at the base opening, and plasticity of concrete occurs locally at the wall corners. Therefore, the height of confinement reinforcement required in a rocking wall is much smaller than that in a special structural wall.

Critical height h_{cr} , over which nonlinear behavior of the concrete in compression is expected to extend, was proposed by other researchers in developing height of the first concrete fiber located

in wall corners at the wall-foundation interface in numerical models. The term “ h_{cr} ” is similar to height of confinement reinforcement (h_{cc}), because confinement reinforcement provides passive confinement effect; that is, it only becomes effective when the confined concrete becomes nonlinear. The expressions developed for h_{cr} include: $h_{cr} = \min(2t'', 2c'')$ (Perez, 2004); $h_{cr} = c$ (Restrepo and Rahman, 2007); $h_{cr} = 0.06H$ (Aaleti and Sritharan 2011); $h_{cr} = \min(1.5t, c)$ (Gavridou et al., 2017), where t and c are thickness and neutral axis depth of the wall measured from end of the wall (t'' and c'' are measured from centerline of confinement reinforcement), H is height of the wall.

Maximum strain in extreme concrete compression fiber ϵ_{cc} - Fig. 7(a) illustrates the deformation of a rocking wall at its corner with a stronger grout bed. The wall is assumed to rock as a rigid body about its corner and not penetrate the stronger grout, thus shortening of the wall ($\theta c''$) is assumed to occur above the grout, where θ is rotation of the wall. Fig. 7(b) shows an approximate concrete compressive-strain distribution along the height of the wall. As described above, the strain decreases rapidly between the base and the cut-off section, where the largest concrete compressive strain decreases to $3000 \mu\epsilon$ and confinement reinforcement is no longer required. It is assumed that the strain within the confined concrete region mainly contributes to the shortening of the wall ($\theta c''$), which is a local behavior as verified by the tests.

Most of the existing research assumed ϵ_{cc} was constant over the critical height (h_{cr}), as shown in Fig. 7(c). The ϵ_{cc} , which was calculated as $\theta c''/h_{cr}$ using the expressions presented above for h_{cr} , is listed in Table 2. As shown in the table, the ϵ_{cc} calculated based on the h_{cr} suggested by Perez and Gavridou et al. provides a reasonable estimation for the “NCREE” and “E-DEFENSE” tests, but it overestimates the strain demand for the “LEHIGH” test (large c due to high axial-

compression ratio and then t decides h_{cr}), which would require an impractical amount of confinement reinforcement to satisfy the demand; the ϵ_{cc} calculated based on the h_{cr} suggested by Aaleti and Sritharan provides the best estimation for the “LEHIGH” and “NCREE” test, but it underestimates the strain demand for the “E-DEFENSE” test, where h_{cr} is large due to the large wall height H_w ; the ϵ_{cc} calculated based on the h_{cr} suggested by Restrepo and Rahman, which makes ϵ_{cc} equal to the target drift θ , provides a reasonable estimation for the “NCREE” and the “E-DEFENSE” test, but it underestimates the strain demand for the “LEHIGH” test.

It should be noted that either $h_{cc} = \max(2t, 1.5c'')$ as proposed in this paper or h_{cr} (related to t_w, t_w'', c, c'' or H_w) as used in other research is empirical in nature and more studies are needed to prove or refine this recommendation further. However, the assumption of constant strain distribution over h_{cr} does not reflect the steep change in strains in wall corners. If the concrete compressive strain is assumed to decrease linearly over the height of confinement reinforcement (h_{cc}) as shown in Fig. 7(c), which is simplified compared to the actual strain distribution shown in Fig. 7(b), the maximum strain in extreme concrete compression fiber at the base (ϵ_{cc}) can be deduced as:

$$\frac{\epsilon_{cc} + 0.003}{2} h_{cc} = \theta c'' \rightarrow \quad (\text{Eq. 1})$$

$$\epsilon_{cc} = \frac{2\theta c''}{h_{cc}} - 0.003 = \frac{2\theta c''}{\max(2t, 1.5c'')} - 0.003$$

Using the data from the three referenced tests, the $\epsilon_{c,pre}$ predicted by Eq. 1 is presented in Table 2. For example, the target drift in the “NCREE” test was 3%, $\epsilon_{cc} = 2 \times 0.03 \times 9.8 / \max(2 \times 6, 1.5 \times 9.8) - 0.003 = 0.037$. As shown in the table, the $\epsilon_{c,pre}$ predicted by Eq. 1 is mostly

larger than that measured in the referenced tests except the “LEHIGH” test, where it is slightly smaller. The proposed Eq. 1 provides a reasonable estimation of the concrete compressive-strain demand at the target drift. It also reflects the test observation that development of ϵ_{cc} at the wall corners was closely related to the lateral drift of the wall (θ) after inelastic compressive strains had been developed in the concrete.

Volumetric ratio of confinement reinforcement ρ_s - Once ϵ_{cc} is obtained through Eq. 1, the required amount of confinement reinforcement can be calculated assuming ϵ_{cc} was achieved when confinement reinforcement fractured (ACI-550.7). If this assumption is adopted with 0.003 as the maximum usable compressive strain of unconfined concrete, the following is attained by rearranging Eq. (6-5) in ACI-550.7:

$$\rho_s = \frac{(\epsilon_{cc} - 0.003)f'_{cc}}{\alpha f_{yt} \epsilon_{su}} \quad (\text{Eq. 2})$$

where, ρ_s = Volumetric ratio of confinement reinforcement to confined concrete core (for circular hoops or spiral, it is equal to the ratio of volume of circular hoops or spiral to that of confined core; for rectangular hoops, it is equal to the sum of confinement ratio in two orthogonal directions), α = Constants for different types of confinement reinforcement (2.07 for circular hoops or spiral, 1.61 for rectangular hoops, Section 6.6.3.8(b) in ACI-550.7), f_{yt} = Yield strength of confinement reinforcement, ϵ_{su} = Ultimate strain of confinement reinforcement, which can be taken as 0.09 considering low-cycle fatigue (ASCE 41-17).

An example is provided for a rocking wall using 80 ksi rectangular hoops and 6 ksi concrete with 3% target drift, assuming $h_{cc} = 1.5c$ ". Based on Eq. 1, $\epsilon_{cc} = 2 \times 0.03c" / (1.5c") - 0.003 = 0.037$. If the hoops are designed to achieve $f'_{cc} = 1.6f'_c$, the required $\rho_s = (0.037 -$

$0.003) \times 1.6 \times 6 / (1.61 \times 80 \times 0.09) = 0.028$. Compared to the requirement for a special structural wall in ACI 318, assuming the confinement ratio is the same in two orthogonal directions and the equation (b) in Table 18.10.6.4(g) governs the design, $\rho_s = 2 \times 0.09 f'_c / f_{yt} = 0.18 \times 6 / 80 \approx 0.014$. The volumetric ratio of confinement reinforcement designed by Eq. 1 for a rocking wall is about twice that for a special structural wall. The constructability of confinement reinforcement should be examined during design to avoid congestion in the wall corners. It is noteworthy that the total quantity of confinement reinforcement required for a rocking wall might not be larger than that for a special structural, because the height of confinement reinforcement required for a rocking wall is much smaller than that for a special structural wall as described above (e.g., 14.7 in. [373 mm] for a rocking wall; 72 in. [1829 mm] for a special structural wall).

In summary, the height and the volumetric ratio of confinement reinforcement required for a rocking wall with stronger grout, which are important design parameters but not included in current design guideline ACI-550.7, can be obtained by using Eq. 1 and Eq. 2 with $h_{cc} = \max (2t, 1.5c)$.

Aspect ratio and shear-sliding resistance – Fig. 8 shows a sketch of a multi-story rocking wall under lateral loads with an inverted-triangular-distributed pattern assumed. In the figure, f is the lateral load on the first level, n is the number of stories, h is the story height, H and W are the overall height and length of the wall, N is the total axial load on the wall (including prestressing forces and sustained gravity loads; considering appropriate load combinations in Table 5.3.1 in ACI 318-19). Shear-sliding resistance of the wall is ϕR_n , where strength reduction factor ϕ is equal to 0.75 per Table 21.2.1 in ACI 318. R_n is the nominal shear-sliding resistance of the wall, which is equal to the total axial load (N) times coefficient of friction (μ). Per ACI-550.7 Section 6.5.3, μ

is 0.5. For the lateral loads distributed on the wall, the moment demand on the wall at the base (M_u) is calculated:

$$M_u = f * h + 2f * 2h + \dots + nf * nh = fh \left[\frac{n(n+1)(2n+1)}{6} \right] \quad (\text{Eq. 3})$$

$$f = \left[\frac{6M_u}{H(n+1)(2n+1)} \right] \quad (\text{Eq. 4})$$

The shear demand on the wall (V_u) is calculated with Eq. 4 substituting f :

$$V_u = f + 2f + \dots + nf = f \frac{n(n+1)}{2} = \frac{3M_u}{H} * \frac{n}{2n+1} \quad (\text{Eq. 5})$$

The probable flexural strength of the rocking wall (M_{pr}) is generated by the total axial load in the wall (N). With action line of N being in the middle of the wall, M_{pr} can be calculated assuming the resultant compressive force acting at the corner of the wall for simplicity:

$$M_{pr} = \frac{N * W}{2} \quad (\text{Eq. 6})$$

Substituting M_u with M_{pr} in Eq. 5, the maximum shear demand on the wall is:

$$V_u = \frac{3M_{pr}}{H} * \frac{n}{2n+1} = \frac{3N * W}{2H} * \frac{n}{2n+1} \quad (\text{Eq. 7})$$

To resist shear-sliding of the wall:

$$\phi R_n > V_u \quad (\text{Eq. 8})$$

$$\phi R_n = \phi \mu N = 0.75 \times 0.5N = 0.375N > \frac{3N * W}{2H} * \frac{n}{2n+1} \quad (\text{Eq. 9})$$

$$\frac{H}{W} > \frac{4n}{2n+1} \quad (\text{Eq. 10})$$

It is noteworthy that by neglecting the existence of neutral axis depth and assuming $W/2$ as the lever arm for N in Eq. 6, a larger V_u is generated in Eq. 7, eventually making the requirement for aspect ratio in Eq. 10 slightly conservative. The aspect ratio of the rocking wall shall satisfy Eq. 10 to resist shear sliding of the wall. The equation provides a stricter requirement compared to ACI-550.7, where minimum 0.5 is recommended. For example, for a 3-story building, the aspect ratio should be larger than 1.7. It is noteworthy that the deduction above is based on the assumption that the rocking wall itself can resist shear-sliding. If other supplemental details are used, such as placing the wall in a foundation pocket (Fig. 2) or adding external shear keys adjacent to the ends of the walls (used in the “DSDM” project, Schoettler 2010), this requirement for the aspect ratio of rocking walls can be relaxed.

Conclusions

By reviewing current design guidelines (ACI-550.7 and ACI 318) and existing experimental studies, some shortcomings in the design parameters of rocking walls (grout bearing, height and volumetric ratio of confinement reinforcement, and aspect ratio) were identified. In this paper, a number of rocking-wall projects are studied, including the “LEHIGH,” “DSDM,” “NCREE,” “E-DEFENSE” tests, and an experimental program of two rocking-wall specimens conducted by the authors (“PFS1” and “PFS2”). The data measured from the wall panels in “PFS1” and “PFS2” were used to study the force flow and the failure mechanism of rocking walls. Based on data analyses of these two tests as well as other referenced tests, and theoretical deduction of the structural behavior, the following conclusions are made:

1. A disturbed region exists at the wall base, where the concentrated compression force distributes rapidly across the length of the wall with height. Correspondingly, the

compressive strains in concrete greatly decrease along the height of the wall due to increased neutral axis depth of the wall.

2. Results from the “PFS1,” “PFS2” and “DSDM” tests show that the development of concrete compressive strains in the walls with weaker grout was not significant and confinement reinforcement was not very effective at 3% drift, which is the drift limit for rocking walls under maximum considered earthquakes per design guideline ACI-550.7. Ductile grout materials weaker than concrete in rocking walls are reasonable alternatives to ACI-550.7 as long as their integrity can be maintained (e.g., incorporating fibers in the grout).
3. Placing confinement reinforcement over a large height in rocking walls with either weaker or stronger grout is not effective, because strain concentration in concrete is a local effect at wall corners and yielding of longitudinal reinforcement is not a concern for rocking walls. It is recommended to place confinement reinforcement over a height not less than 2 times wall thickness or 1.5 times neutral axis depth of the wall at target drifts.
4. Based on the data collected from the existing tests (“LEHIGH”, “NCREE” and “E-DEFENSE”) with stronger grout, an equation, which is related to the target drift, neutral axis depth of the wall, and height of the confinement reinforcement, is proposed to determine maximum strain in extreme concrete compression fiber. It serves as the basis to determine the volumetric ratio of the confinement reinforcement at the corners of rocking walls.

5. An equation limiting aspect ratio of rocking walls is proposed to ensure the walls are capable of resisting shear sliding without additional sources of resistance (e.g., shear keys). The requirement is stricter than that in ACI-550.7 (i.e., minimum 0.5 is not sufficient).

References

1. Aaleti, S., and Sritharan, S. (2011). "Performance Verification of the PreWEC Concept and Development of Seismic Design Guidelines." *ISU-ERI-Ames Report ERI-10347*, Iowa State University, Ames, IA
2. ACI (American Concrete Institute). (2009). Requirements for Design of a Special Unbonded Post-Tensioned Precast Shear Wall Satisfying ACI-550.6 (ACI 550.7) and Commentary. *ACI 550.7*, Farmington Hills, MI.
3. ACI (American Concrete Institute). (2104, 2019). "Building code requirement for reinforced concrete." *ACI 318-14, ACI 318-19*, Farmington Hills, MI
4. ASCE (American Society of Civil Engineers). (2017). "Seismic Evaluation and Retrofit of Existing Buildings." *ASCE/SEI 41-17*, Reston, VA
5. Belleri, A., Schoettler, M.J., Restrepo, J.I., and Fleischman, R.B. (2014). "Dynamic Behavior of Rocking and Hybrid Cantilever Walls in a Precast Concrete Building." *ACI Struct. J.*, 111(3), 661–671.
6. Henry, R. S. (2011). "Self-centering Precast Concrete Walls for Buildings in Regions with Low to High Seismicity," Ph.D. thesis, University of Auckland, New Zealand
7. Gavridou, S., Wallace, J. W., Nagae, T., Matsumori, T., Tahara, K., and Fukuyama, K. (2017). "Shake-Table Test of a Full-Scale 4-Story Precast Concrete Building. I: Overview and Experimental Results." *J. Struct. Eng.*, 143(6).

8. Gavridou, S., Wallace, J. W., Nagee, T., Matsumori, T., Tahara, K., and Fukuyama, K. (2017). "Shake-Table Test of a Full-Scale 4-Story Precast Concrete Building. II: Analytical Studies." *J. Struct. Eng.*, 143(6).
9. Liu, Q. Z. (2016). "Study on Interaction between Rocking-Wall System and Surrounding Structure." *Ph.D. thesis*, Univ. of Minnesota, Twin Cities, Minnesota, the United States
10. Perez, F. K. (2004). "Experimental and Analytical Lateral Load Response of Unbonded Post-Tensioned Precast Concrete Walls" *Ph.D. thesis*, Lehigh University, Pennsylvania
11. Priestley, M.J.N., Sritharan, S., Conley, J., and Pampanin, S. (1999). "Preliminary results and conclusions from the PRESSS five-story precast concrete test buildings." *PCI J.*, 44(6), 42-67
12. Restrepo, J. I., and Rahman, M. A. (2007). "Seismic Performance of Self-Centering Structural Walls Incorporating Energy Dissipators." *J. Struct. Eng.*, 133(11), 1560-1570
13. Schoettler M.J. (2010). "Seismic Demands in Precast Concrete Diaphragms," *Ph.D. thesis*, University of California, San Diego, San Diego, CA
14. Smith, B. (2012). "Design, Analysis, and Experimental Evaluation of Hybrid Precast Concrete Shear Walls for Seismic Regions.", *Ph.D. thesis*, Dept. of Civil Engineering and Geological Sciences, Univ. of Notre Dame, Notre Dame, Indiana, the United States

TABLES AND FIGURES

LIST OF TABLES:

Table 1 Summary of design details in current code and existing tests (1 in. = 25.4 mm)

Table 2 Summary of test observations and strain data from existing tests at target drifts with stronger grout (1 in. = 25.4 mm)

LIST OF FIGURES:

Fig. 1 - Design parameters of rocking walls

Fig. 2 - Concrete (CG) and steel (SG) strain gages in the rocking walls

Fig. 3 - Concrete compressive-strain distribution along length of the wall

Fig. 4 - Concrete compressive-strain distribution along height of the wall

Fig. 5 - Stirrup strain along height of wall

Fig. 6 - Stress distribution and force flow in a rocking wall and a special structural wall

Fig. 7 - Deformation and compressive-strain distribution of rocking walls

Fig. 8 - Shear-sliding resistance of a rocking wall under lateral loads

Table 1 Summary of design details in current code and existing tests (1 in. = 25.4 mm)

Test	Wall			Aspect ratio	Confinement				
	Height in.	Length in.	Thickness in.		Volumetric ratio	Length in.	Height in.	Height/ Wall Length	Height/ Wall Height
ACI-550.7	-	-	-	Minimum 0.5	NA	Minimum of (0.95c, 12 in.)	NA	NA	NA
LEHIGH	284.8	100	6	2.8	0.074	26.75	65	0.65	0.23
DSDM	276	96	8	2.9	0.028	11	30	0.31	0.11
NCREE	230.6	72	6	3.2	0.068	14.5	72	1.0	0.31
E-DEFENSE	488.2	98.4	9.8	5.0	0.054	21	41	0.42	0.08
PFS1	224	90	6	2.5	0.034	13	42	0.47	0.19
PFS2	219	68	6	3.2	0.031	12	38	0.56	0.17

Table 2 Summary of test observations and strain data from existing tests at target drifts with stronger grout (1 in. = 25.4 mm)

Test	Δ (in.)	t (in.)	c'' (in.)	h_{cc} (in.)	$\varepsilon_{cc,measured}$		ε_t		Target Drift (%)	$\varepsilon_{c,pre} (\mu\varepsilon)$				
					Value ($\mu\varepsilon$)	Height (in.)	Value ($\mu\varepsilon$)	Height (in.)		Eq. 1	Perez	Restrepo Rahman	Sritharan el al.	Gavridou et al.
LEHIGH	15	6	21.3	32	-45000* -15400 -6900 -2680	4.75 9 20.25 32.5	NA		3.5	-43670	-93190	-35000	-44050	-82830
NCREE	10	6	9.8	14.7	-15000 -2080	5 15	1800 560	5.9 13	3	-37000	-30150	-30000	-21520	-32670
E- DEFENSE	9.8	9.8	6.9	19.6	-23000 -15000 -1000	4.9 9.9 19.7	240	12.6	3	-37000	-26540	-30000	-7210	-30000

*: Negative sign represents compressive strains.

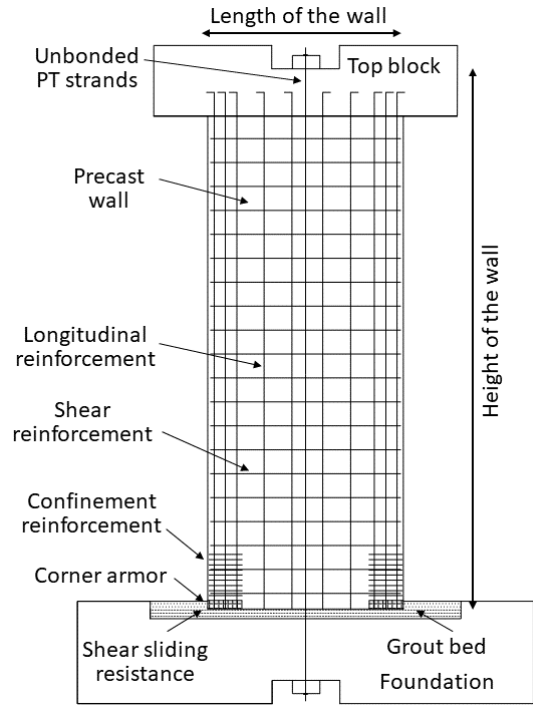
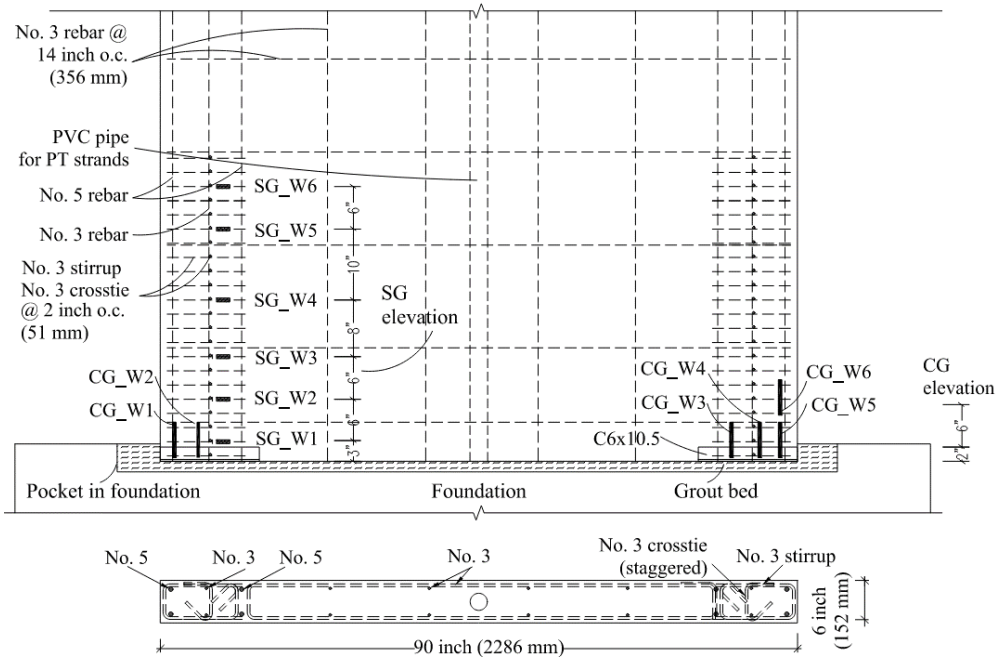
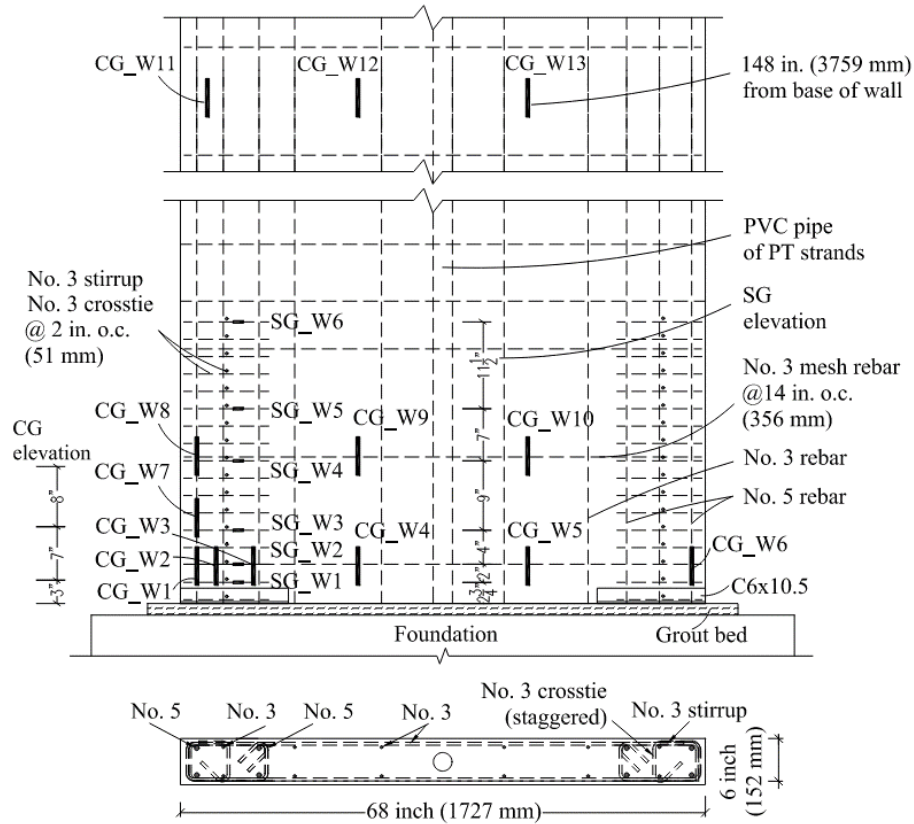


Fig. 1 Design parameters of rocking walls

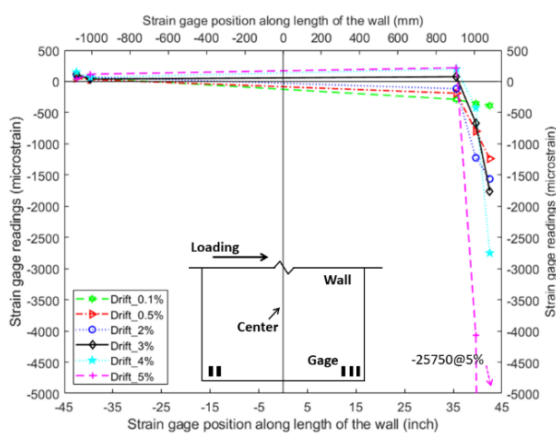


(a) PFS1

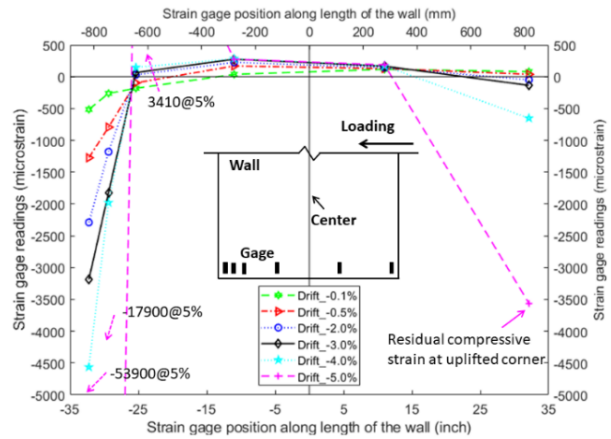


(b) PFS2

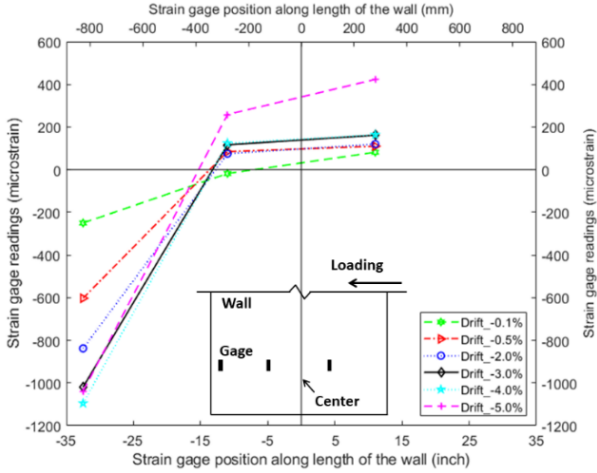
Fig. 2 Concrete (CG) and steel (SG) strain gages in the rocking walls



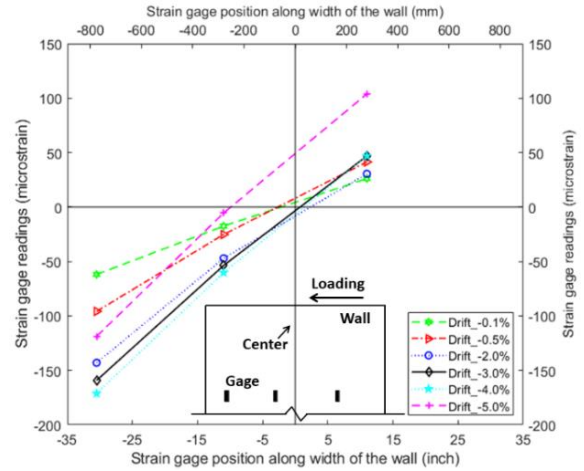
(a) Near wall base in PFS1



(b) Near wall base in PFS2

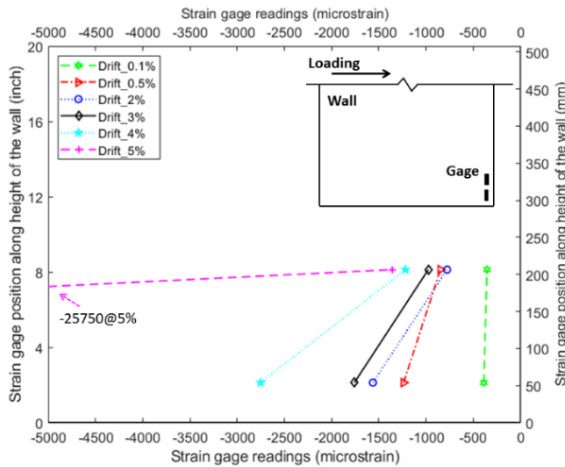


(c) At the second row of gages in PFS2

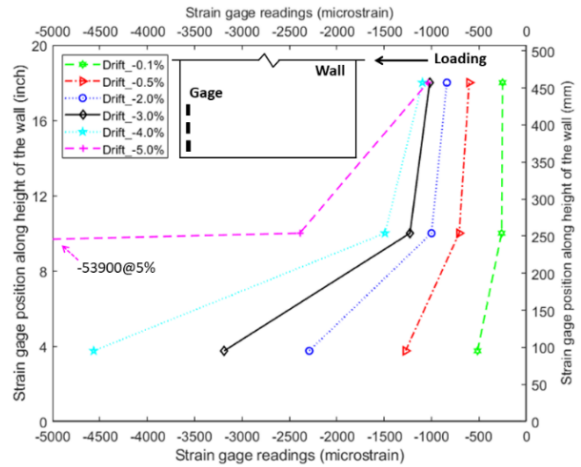


(d) At the third row of gages in PFS2

Fig. 3 Concrete compressive-strain distribution along length of the wall

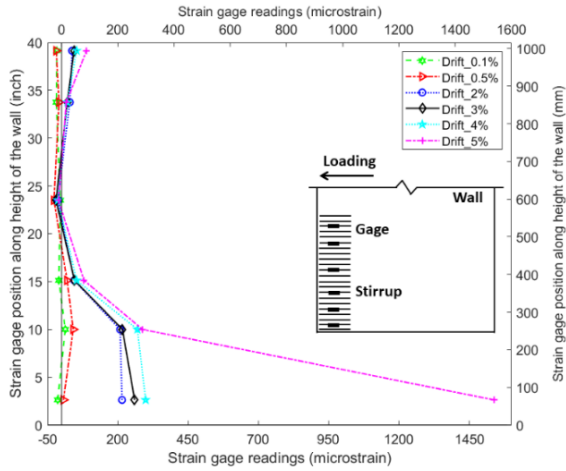


(a) Within 10 in. from base in PFS1

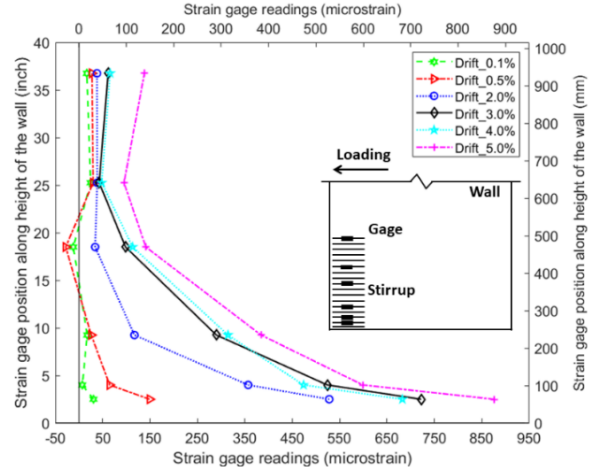


(b) Within 18 in. from base in PFS2

Fig. 4 Concrete compressive-strain distribution along height of the wall

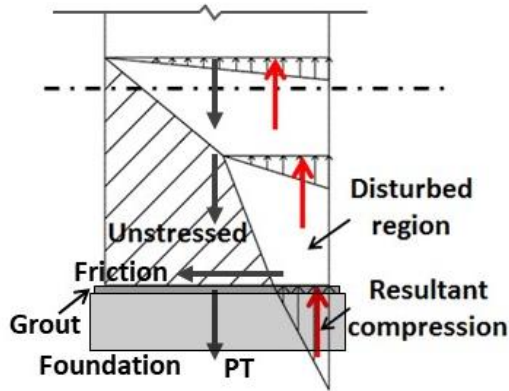


(a) PFS1

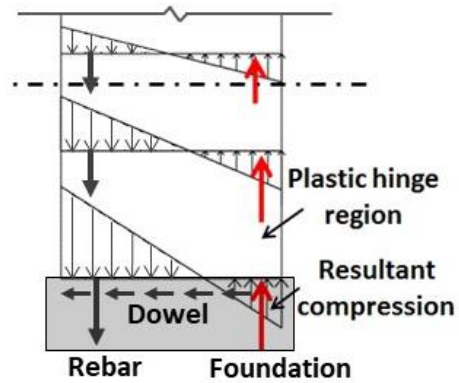


(b) PFS2

Fig. 5 Stirrup strain along height of wall

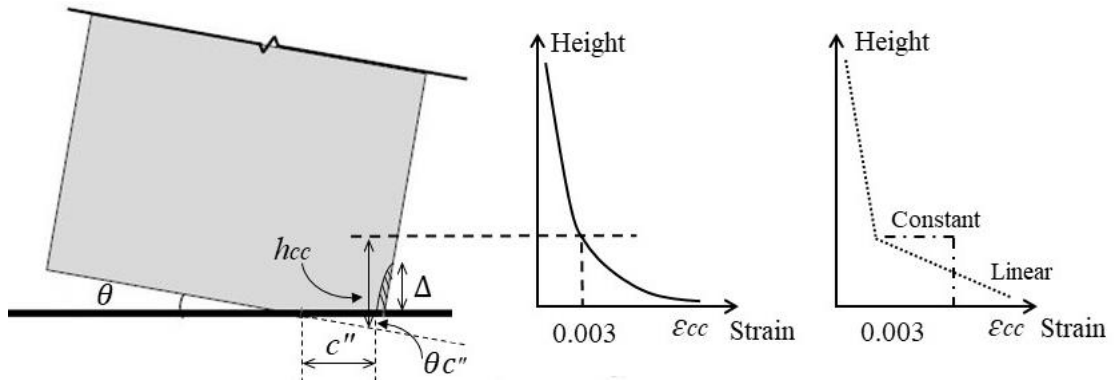


(a) Rocking wall



(b) Special structural wall

Fig. 6 Stress distribution and force flow in a rocking wall and a special structural wall



(a) Wall deformation (b) Actual distribution (c) Simplified distribution

Fig. 7 Deformation and compressive-strain distribution of rocking walls

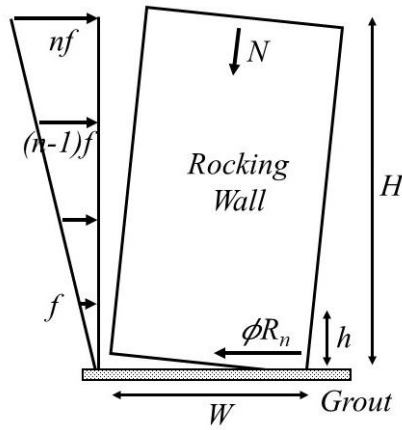


Fig. 8 Shear-sliding resistance of a rocking wall under lateral loads